Supplementary Information

Influence of crystallization solvents on the crystal structures and supramolecular assemblies of [2]naphthyl-extended pillar[6]arene

Randa Abd Almoaeen, Mickey Vinodh, Fatemeh H. Alipour and Talal F. Al-Azemi*

Chemistry Department, Kuwait University, P.O. Box 5969, Safat 13060, Kuwait.

Table of contents

Table S1. Summary on the nature and various crystallographic parameters of **[2]Naph-ExP6.CH_2Cl_2**, **[2]Naph-ExP6.EtOAc, [2]Naph-ExP6.DMF** and **Naph-ExP6.PhMe** obtained after crystallization.

Crystal sample	**[2]Naph-ExP6.CH_2Cl_2**	**[2]Naph-ExP6.EtOAc**	**[2]Naph-ExP6.DMF**	**[2]Naph-ExP6.PhMe**
Chemical formula	$C_{60}H_{60}Cl_4O_8$	$C_{66}H_{72}O_{12}$	$C_{61}H_{63}NO_9$	$C_{65}H_{64}O_8$
M_r	1050.88	1057.23	954.12	973.16
Crystal system, space group	Triclinic, *P*-1	Triclinic, *P*-1	Triclinic, *P*-1	Monoclinic, *C*2/*c*
Temperature (K)	150	150	150	150
a, *b*, *c* (Å)	9.1874 (11), 12.0093 (15), 13.4058 (17)	7.6632 (8), 14.3047 (12), 14.6009 (14)	6.1503 (7), 14.6468 (17), 15.6536 (16)	8.3064 (14), 26.469 (4), 23.594 (4)
α, β, γ (°)	67.487 (5), 82.909 (6), 80.060 (6)	114.480 (8), 97.459 (7), 101.331 (7)	108.611 (8), 93.917 (7), 101.669 (7)	90, 95.880 (7), 90
V (Å^3)	1343.2 (3)	1387.7 (2)	1295.3 (3)	5160.0 (14)
Z	1	1	1	4
Radiation type	Mo *K*α	Mo *K*α	Mo *K*α	Mo *K*α
μ (mm^{-1})	0.28	0.09	0.08	0.08
Crystal size (mm)	0.20 × 0.05 × 0.03	0.20 × 0.08 × 0.04	0.20 × 0.07 × 0.06	0.16 × 0.05 × 0.02
Diffractometer	Rigaku R-AXIS RAPID	Rigaku R-AXIS RAPID	Rigaku R-AXIS RAPID	Rigaku R-AXIS RAPID
Absorption correction	Multi-scan *ABSCOR* (Rigaku, 1995)	Multi-scan *ABSCOR* (Rigaku, 1995)	Multi-scan *ABSCOR* (Rigaku, 1995)	Multi-scan *ABSCOR* (Rigaku, 1995)
T_{min}, T_{max}	0.171, 0.996	0.490, 0.997	0.543, 0.995	0.571, 0.998
No. of measured, independent & observed [$I > 2\sigma(I)$] reflections	13389, 4617, 1926	15160, 4817, 2922	14986, 4462, 2599	15146, 4538, 1642
R_{int}	0.104	0.060	0.046	0.104
$(\sin\theta/\lambda)_{max}$ (Å^{-1})	0.595	0.595	0.595	0.595
$R[F^2 > 2\sigma(F^2)]$, $wR(F^2)$, S	0.083, 0.281, 0.96	0.058, 0.154, 1.02	0.081, 0.269, 1.05	0.109, 0.343, 1.12
No. of reflections	4617	4817	4462	4538
No. of parameters	356	358	347	361
No. of restraints	36	-	99	147

H-atom treatment	Constrained	Constrained	Constrained	Constrained
$\Delta\rho_{max}$, $\Delta\rho_{min}$ (e Å^{-3})	0.36, −0.41	0.34, −0.23	0.30, −0.32	0.54, −0.20

Computer programs: *SHELXL2019*/3.

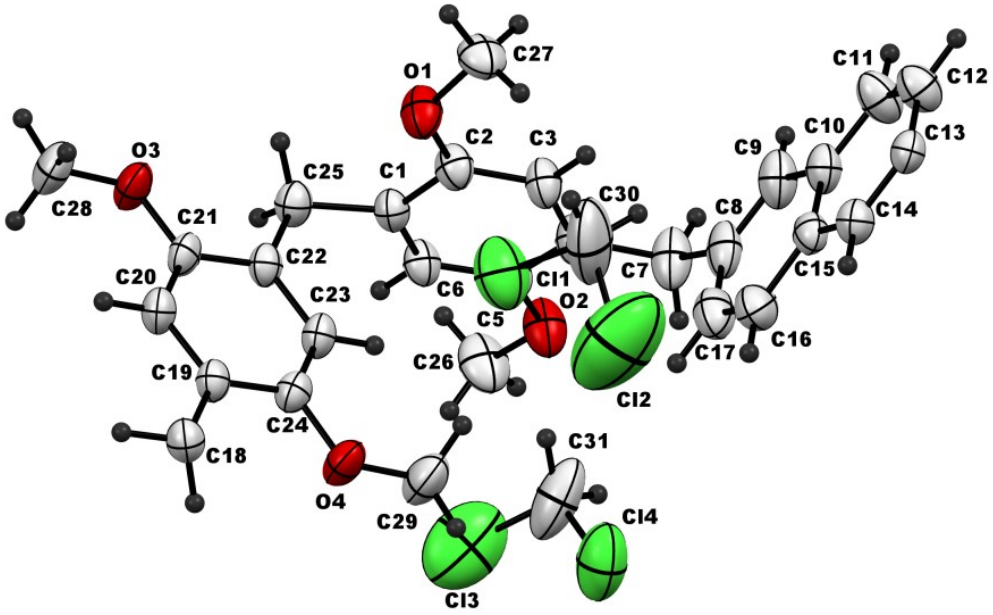

Fig. S1 Thermal ellipsoid representation (30% probability) the asymmetric unit of **[2]Naph-ExP6.CH_2Cl_2**.

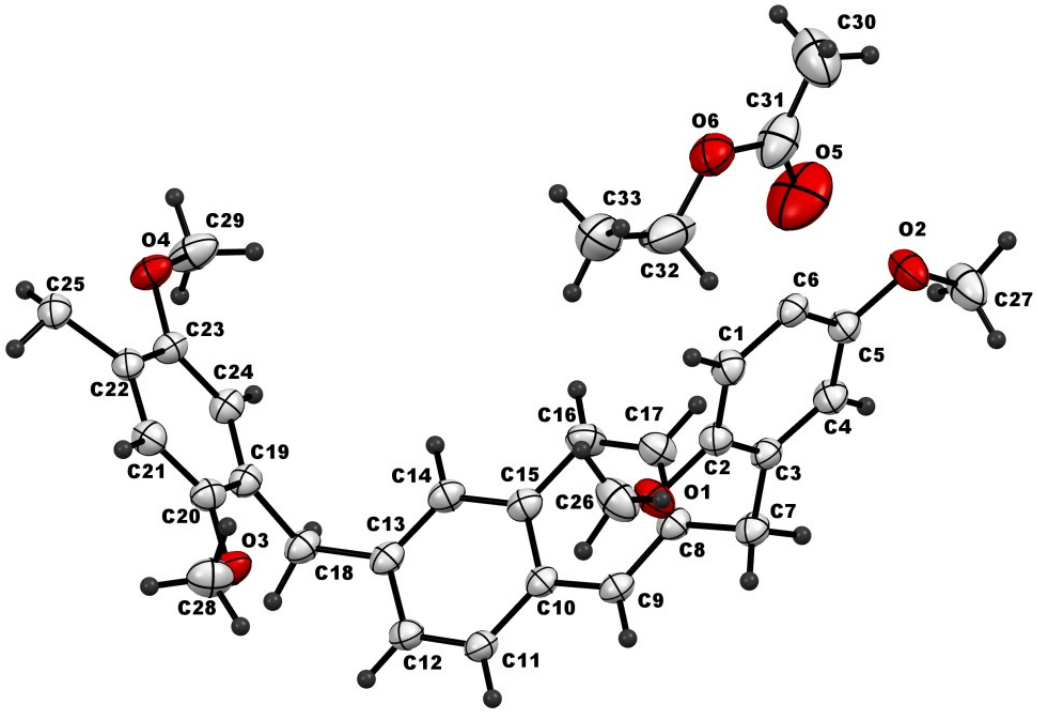

Fig. S2 Thermal ellipsoid representation (30% probability) the asymmetric unit of **[2]Naph-ExP6.EtOAc**.

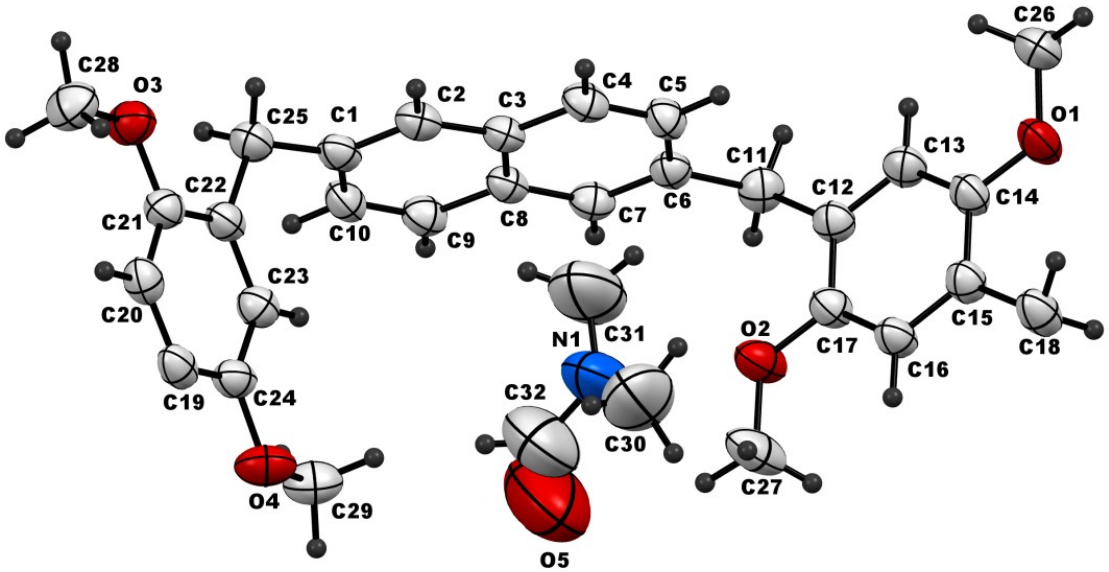

Fig. S3 Thermal ellipsoid representation (30% probability) the asymmetric unit of **[2]Naph-ExP6.DMF**.

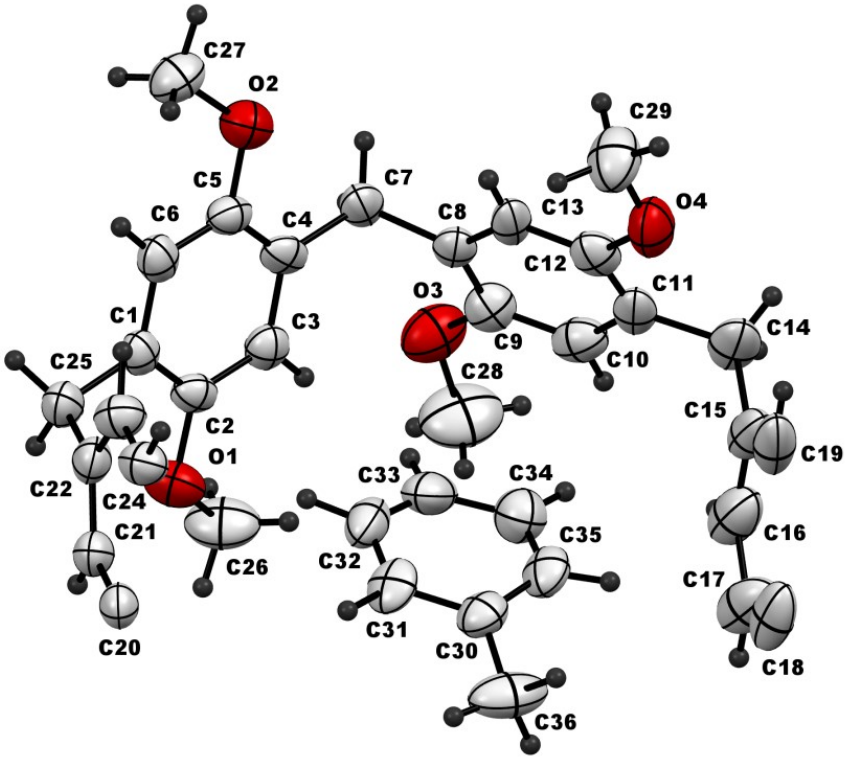

Fig. S4 Thermal ellipsoid representation (30% probability) the asymmetric unit of **[2]Naph-ExP6.PhMe**.

Table S2. Geometric parameters of different [2]naphthyl-extended pillar[6]arene **([2]Naph-ExP6)** systems.

[2]Naph-ExP6 system	**[2]Naph-ExP6. CH_2Cl_2**	**[2]Naph-ExP6. EtOAc**	**[2]Naph-ExP6. DMF**	**[2]Naph-ExP6. PhMe**
Distance between opposite naphthalene units (Å)	9.47	10.84	10.10	9.88
Maximum distance between two opposite vertices (Å)	13.27	13.05	13.51	13.80
Average cavity width (Å)	10.53	11.20	10.94	10.87
Cavity height (Å)	4.35	4.28	4.10	4.64

Table S3. Tilt angles of the aromatic walls relative to the macrocycle mean plane and dihedral angles between aromatic units in different [2]naphthyl-extended pillar[6]arene ([2]**Naph-ExP6**) systems.

[2]Naph-ExP6 system	**[2]Naph-ExP6. CH_2Cl_2**	**[2]Naph-ExP6. EtOAc**	**[2]Naph-ExP6. DMF**	**[2]Naph-ExP6. PhMe**
Tilt angles_ naphthalene rings	47.0° & 133.0°	57.6° & 122.4°	77.0° & 103.0°	90.0 & 90.0
Tilt angles_ phenyl rings (a)	48.5° & 131.5°	55.1° & 124.9°	45.2° & 134.8°	82.2° & 97.8°
Tilt angles_ phenyl rings (b)	51.7° & 128.3°	83.6° & 96.4°	49.2° & 130.8°	59.9° & 120.1°
Dihedral angles_ naphthalene ring Vs phenyl ring (a)	81.1°	89.6°	86.6°	67.6°
Dihedral angles_ naphthalene ring Vs phenyl ring (b)	78.3°	75.8°	78.3°	61.0°
Dihedral angles_ phenyl ring (a) Vs phenyl ring (b)	85.6°	60.6°	84.2°	65.3°

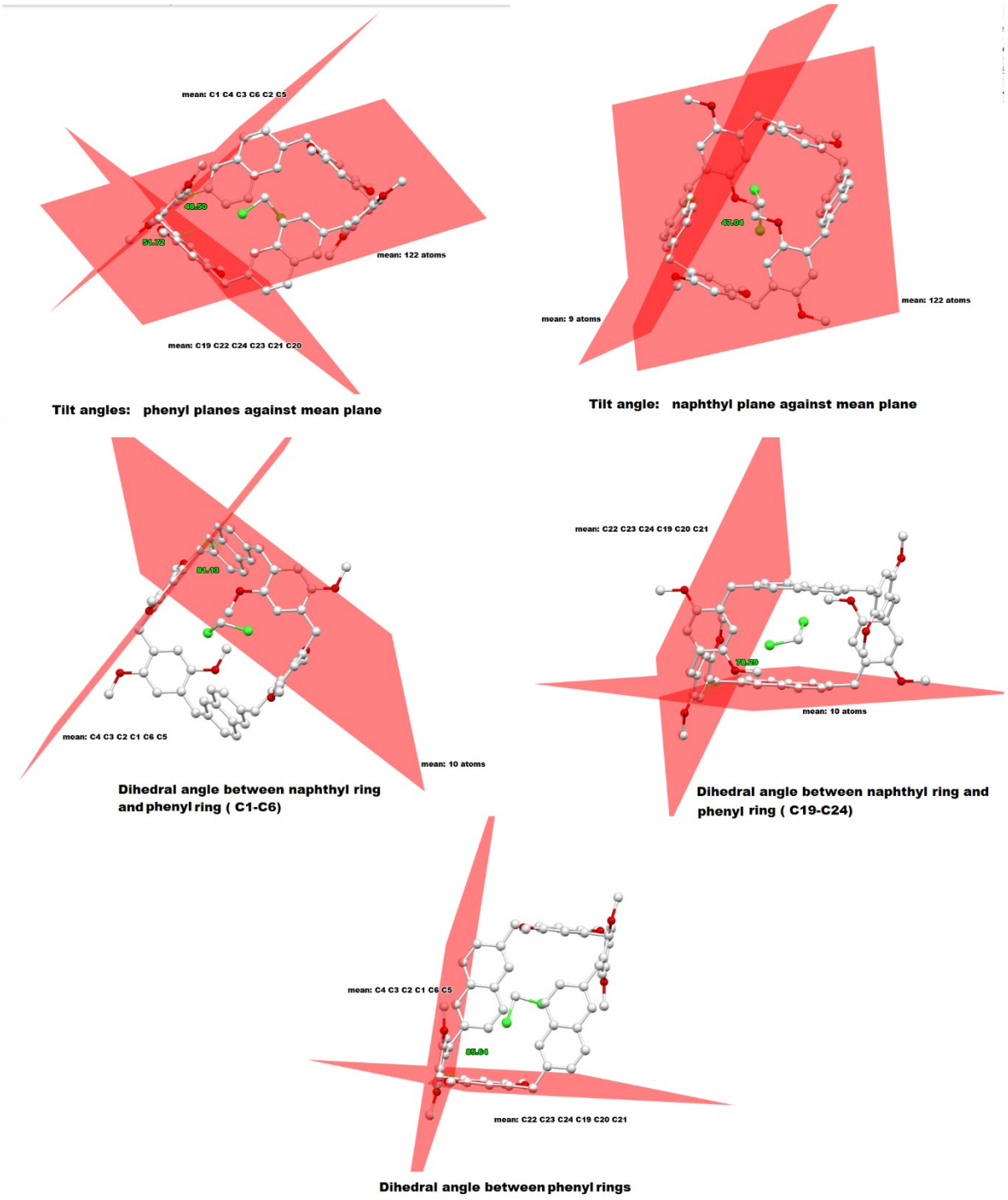

Fig. S5. Tilt angles of the aromatic walls relative to the macrocycle mean plane & dihedral angles between aromatic units in **[2]Naph-ExP6.CH_2Cl_2** system.

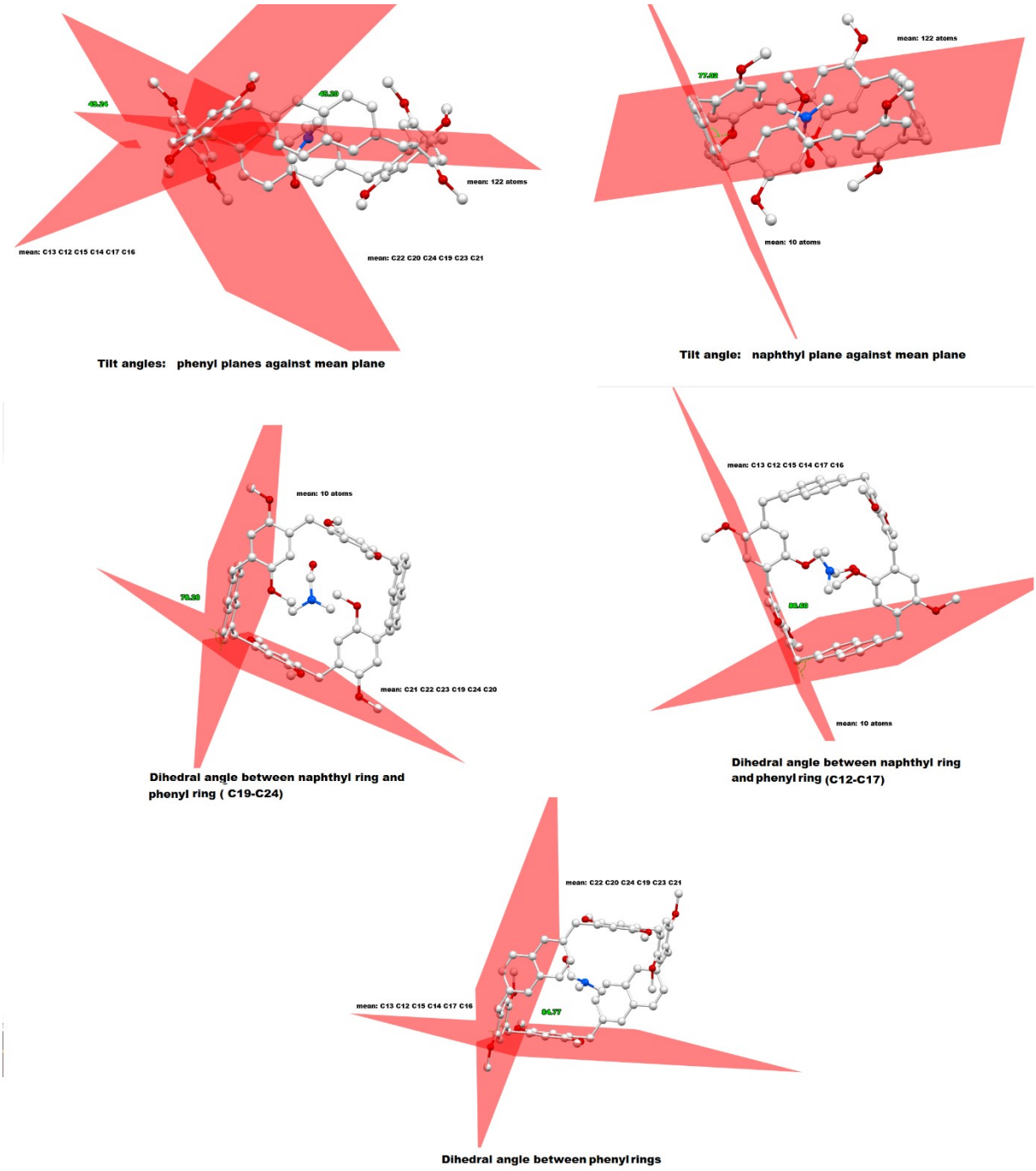

Fig. S6. Tilt angles of the aromatic walls relative to the macrocycle mean plane & dihedral angles between aromatic units in **[2]Naph-ExP6.DMF** system.

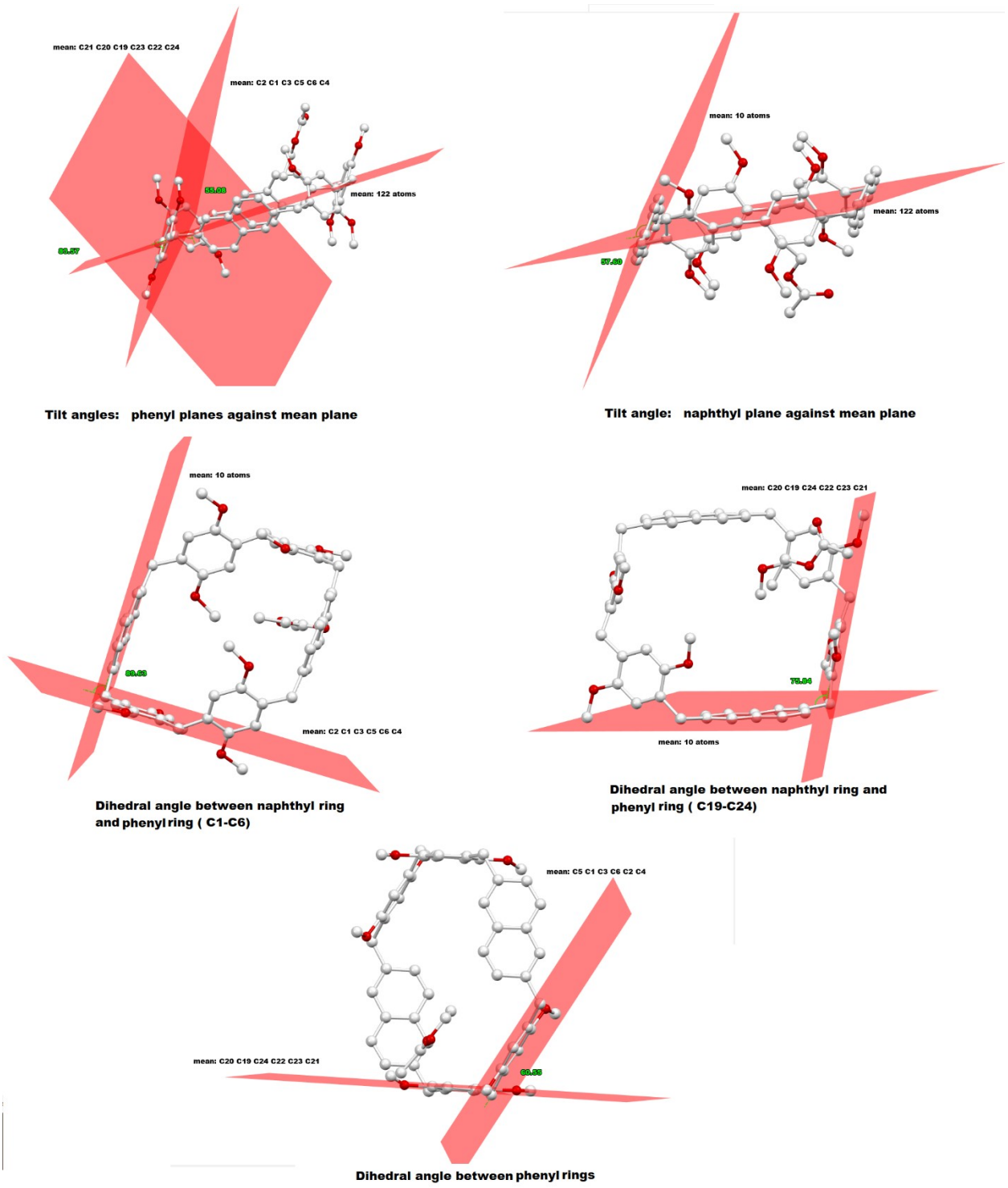

Fig. S7. Tilt angles of the aromatic walls relative to the macrocycle mean plane & dihedral angles between aromatic units in **[2]Naph-ExP6.EtOAc** system.

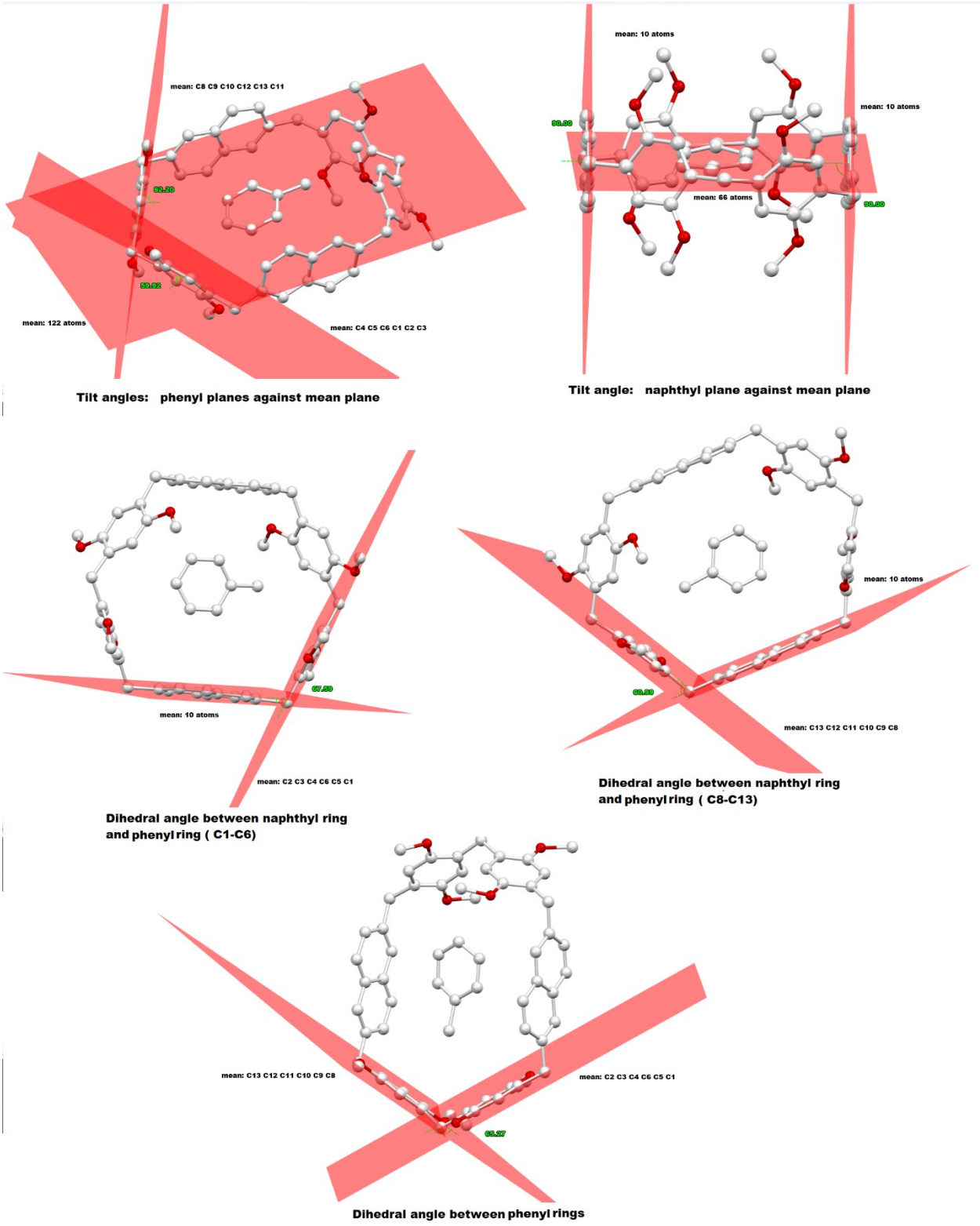

Fig. S8. Tilt angles of the aromatic walls relative to the macrocycle mean plane & dihedral angles between aromatic units in **[2]Naph-ExP6.PhMe** system.

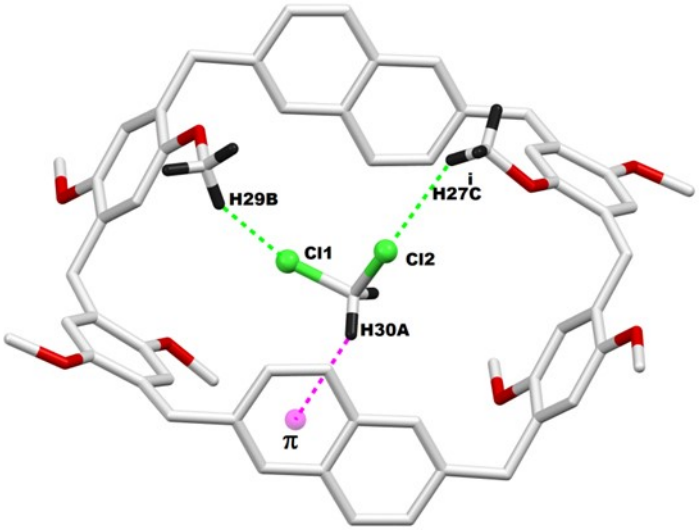

Fig. S9. Host-guest non-bonding interactions in the crystal network of **[2]Naph-ExP6.CH_2Cl_2.** π is the centroid of the aromatic ring constitute C8, C9, C10, C15, C16, C17 atoms; Symmetry code: (i) -x, -y, 1-z.

Table S4. Quantitative details of Host-guest intermolecular non-bonding interactions in the crystal network of **[2]Naph-ExP6.CH_2Cl_2** (Å, °).

A-B···C	**A-B**	**B···C**	**A···C**	**A-B···C**
$C27^{i}$-H27C^{i}···Cl12	0.980	2.79	3.63(1)	144.7
C29-H29B···Cl1	0.980	2.823	3.662(9)	144.0
C30-H30A···π	0.99	3.446	4.281	143.41

π is the centroid of the aromatic ring constitutes C8, C9, C10, C15, C16, C17 atoms; Symmetry code: (i) -x, -y, 1-z.

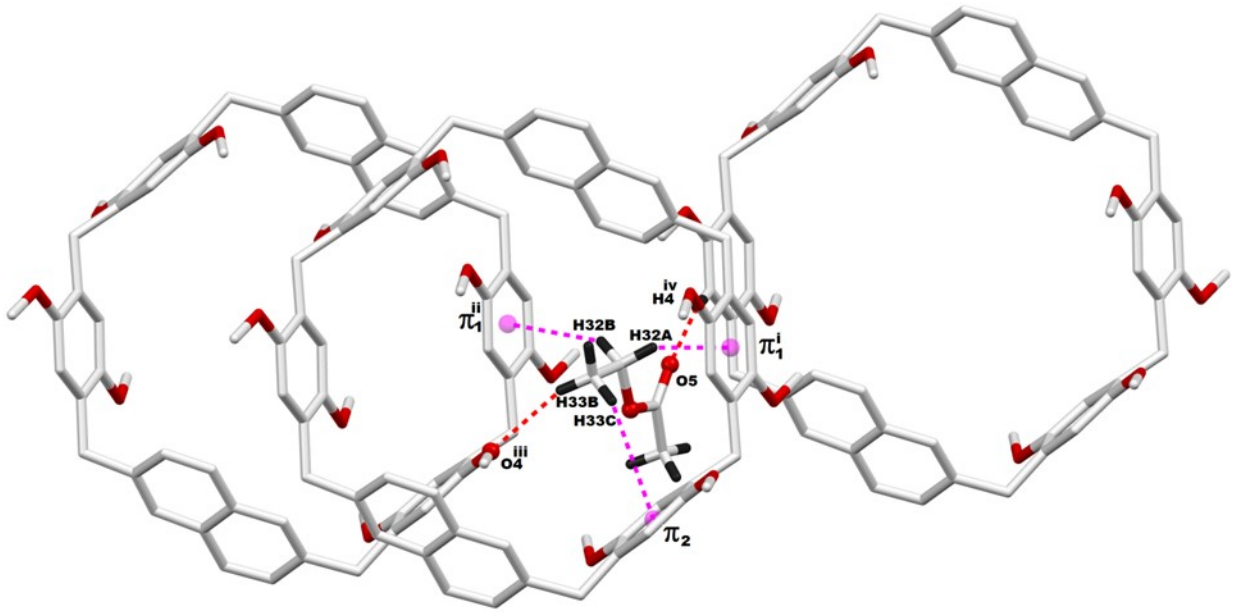

Fig. S10. Host-guest non-bonding interactions in the crystal network of **[2]Naph-ExP6.EtOAc**. π1and π2 are the centroid of the aromatic rings constitute C1- C6 atoms and C19-C24 atoms respectively. Symmetry code: (i) 1-x, -y, 1-z; (ii) -x, -y, 1-z; (iii) -1+x, y, z and (iv) 1+x, 1+y, 1+z.

Table S5. Quantitative details of Host-guest non-bonding interactions in the crystal network of **[2]Naph-ExP6.EtOAc** (Å, °).

A-B···C	**A-B**	**B···C**	**A···C**	**A-B···C**
C4^{iv}-H4^{iv}···O5	0.950	2.463	3.403(4)	169.9
C32-H32A···π1^{i}	0.990	2.930	3.755	141.46
C32-H32B··· π1^{ii}	0.989	3.178	4.057	148.86
C33-H33B···O4^{iii}	0.980	2.590	3.536(6)	162.4
C33-H33C···π2	0.980	3.675	4.614	161.4

π1and π2 are the centroid of the aromatic rings constitute C1- C6 atoms and C19-C24 atoms respectively. Symmetry code: (i) 1-x, -y, 1-z; (ii) -x, -y, 1-z; (iii) -1+x, y, z and (iv) 1+x, 1+y, 1+z.

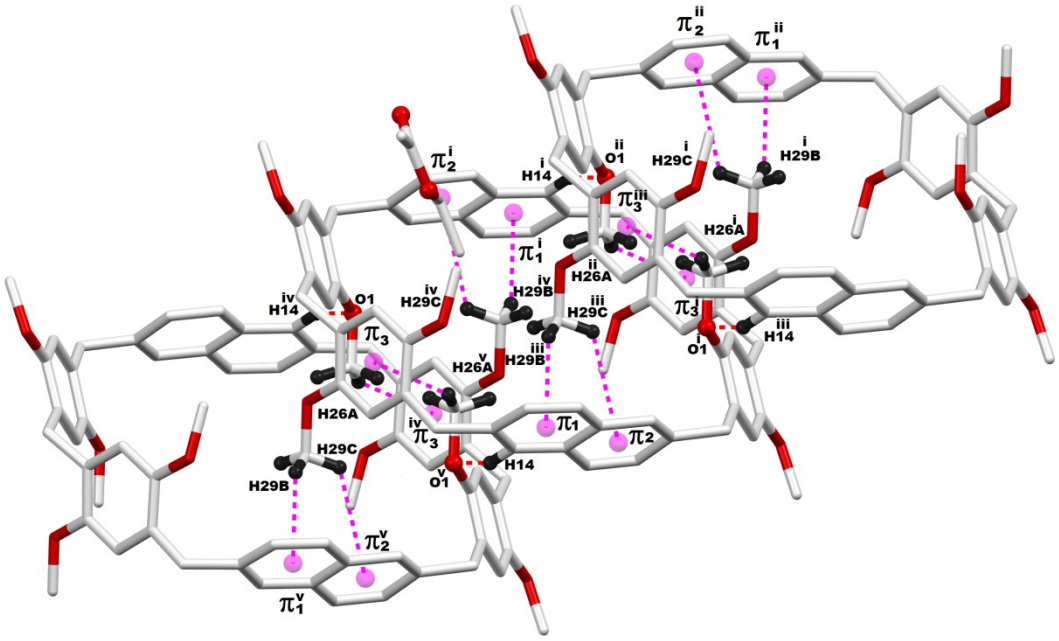

Fig. S11. Intermolecular non-bonding interactions among **[2]Naph-ExP6** molecules in the crystal network of **[2]Naph-ExP6·EtOAc**. π1- π3 are the centroid of the aromatic rings constitute C10-C15 atoms, C8, C9, C10, C15, C16, C17 and C19-C24 atoms respectively; Symmetry code: : (i) 1-x, -y, 1-z; (ii) -x, -y, 1-z; (iii) -1+x, y, z; (iv) 2-x, -y, 1-z and (v) 1+x, y, z.

Table S6. Quantitative details of intermolecular non-bonding interactions among **[2]Naph-ExP6** molecules in the crystal network of **[2]Naph-ExP6.EtOAc**

A-B···C	**A-B**	**B···C**	**A···C**	**A-B···C**
C14-H14···O1^{v}	0.951	2.720	3.560(4)	147.7
C26-H26A··· π3^{iv}	0.980	3.016	3.897	150.17
C29-H29B···π1^{v}	0.980	2.610	3.416	139.66
C29-H29C··· π2^{v}	0.980	3.062	3.610	116.67

π1- π3 are the centroid of the aromatic rings constitute C10- C15 atoms, C8, C9, C10, C15, C16, C17 and C19-C24 atoms respectively. Symmetry code: (iv) 2-x, -y, 1-z and (v) 1+x, y, z.

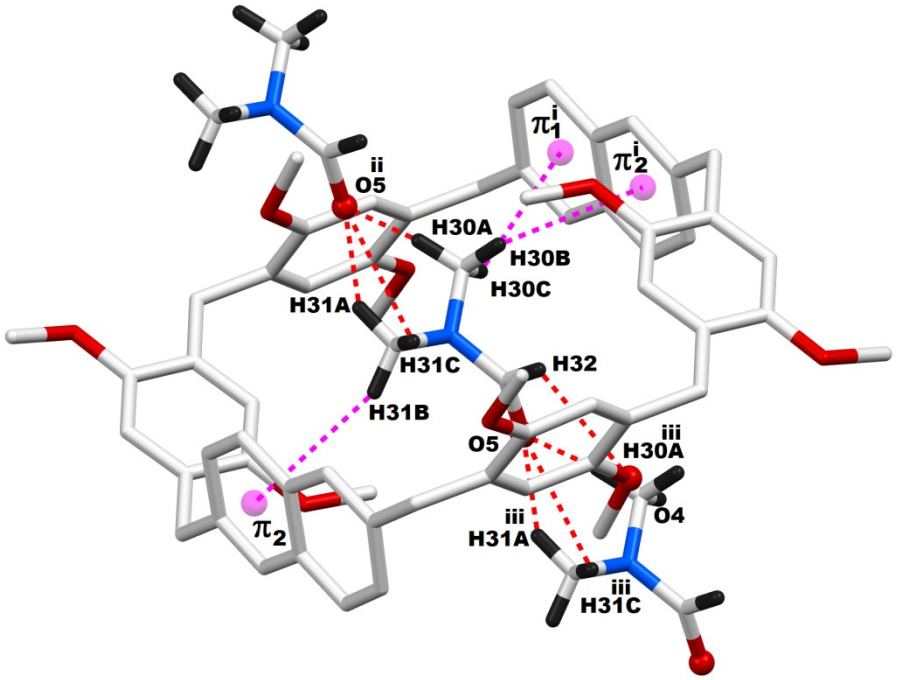

Fig. S12. Host-guest inter molecular non-bonding interactions in the crystal network of **[2]Naph-ExP6.DMF** π1 and π2 are the centroid of the aromatic rings constitute C1, C2, C3,C8, C9, C10 atoms and C3-C8 atoms respectively; Symmetry code: (i) -x, -y, 2-z; (ii) -1+x, y, z and (iii) 1+x, y, z.

Table S7. Quantitative details of Host-guest non-bonding interactions in the crystal network of **[2]Naph-ExP6.DMF** (Å, °).

A-B···C	**A-B**	**B···C**	**A···C**	**A-B···C**
C30-H30A···O5^{ii}	0.98	3.10	3.69(3)	120
C30-H30B···π2^{i}	0.98	3.384	3.879	113.47
C30-H30C···. π1^{i}	0.98	3.360	4.088	132.58
C31-H31A···O5^{ii}	0.98	2.46	3.09(3)	122
C31-H31B···π2	0.98	3.218	4.062	145.49
C31-H31C···. O5^{ii}	0.98	2.87	3.09(3)	94
C32-H32···O4	0.95	3.466	4.16(2)	132

π1 and π2 are the centroid of the aromatic rings constitute C1, C2, C3, C8, C9, C10 atoms and C3-C8 atoms respectively; Symmetry code: (i) -x, -y, 2-z and (ii) -1+x, y, z.

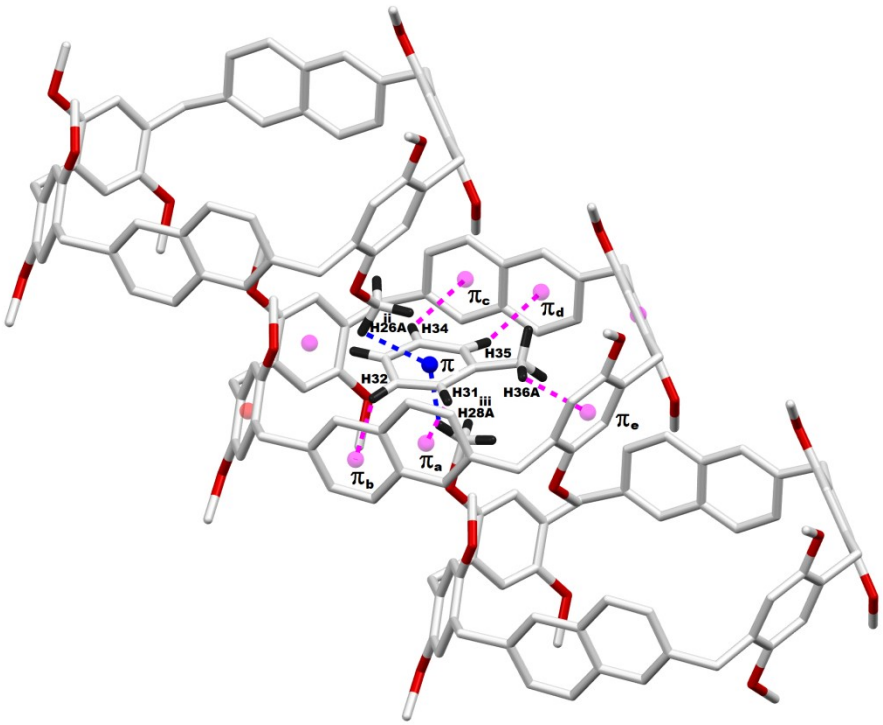

Fig. S13. Host-guest non-bonding interactions in the crystal network of **[2]Naph-ExP6.PhMe.** π is the centroid of toluene aromatic ring; πa to πe are the centroid of the aromatic rings constitute C20, C20^{i}-C24^{i} atoms, C20-C24, C20^{i}, atoms and C15-C19, C18^{i} atoms, C18, C15^{i}-C19^{i} atoms, and C1^{i}-C6^{i} atoms respectively. Symmetry code: (i) -x, y, ½-z; (ii) -1-x, y, 1/2-z and (iii) 1+x, y, z.

Table S8. Quantitative details of Host-guest intermolecular non-bonding interactions in the crystal network of **[2]Naph-ExP6.PhMe (** Å, ^{o}).

A-B···C	**A-B**	**B···C**	**A···C**	**A-B···C**
C31-H31··· πa	0.95	3.200	4.080	154.90
C32-H32··· πb	0.95	3.085	3.890	143.48
C34-H34··· πc	0.95	2.929	3.656	134.38
C35-H35··· πd	0.95	2.864	3.776	161.15
C36-H36B··· πe	0.98	3.286	3.740	110.19
C26^{ii}-H26A^{ii}···π	0.981	3.472	3.831	104.07
C28^{iii}-H28A^{iii}··· π	0.98	3.259	4.047	138.63

π is the centroid of toluene aromatic ring; πa to πe are the centroid of the aromatic rings constitute C20, C20^{i}-C24^{i} atoms, C20-C24, C20^{i}, atoms and C15-C19, C18^{i} atoms, C18, C15^{i}-C19^{i} atoms, and C1^{i}-C6^{i} atoms respectively. Symmetry code: (i) -x, y, ½-z; (ii) -1-x, y, 1/2-z and (iii) 1+x, y, z.

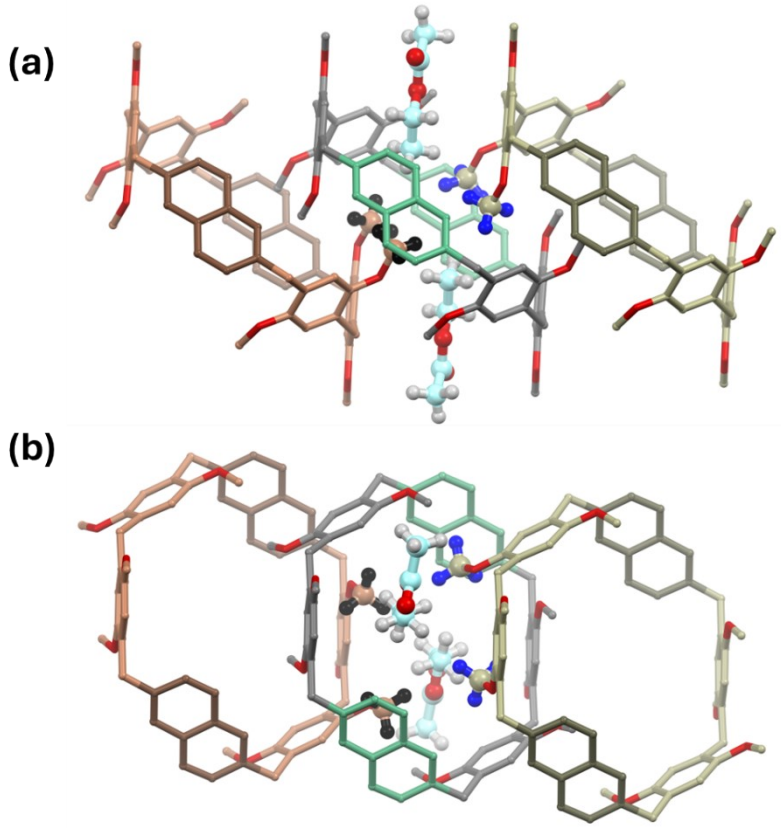

Fig. S14. Crystal structure **[2]Naph-ExP6·EtOAc** interaction with the neighboring macrocycles (a) side view and (b) top view.

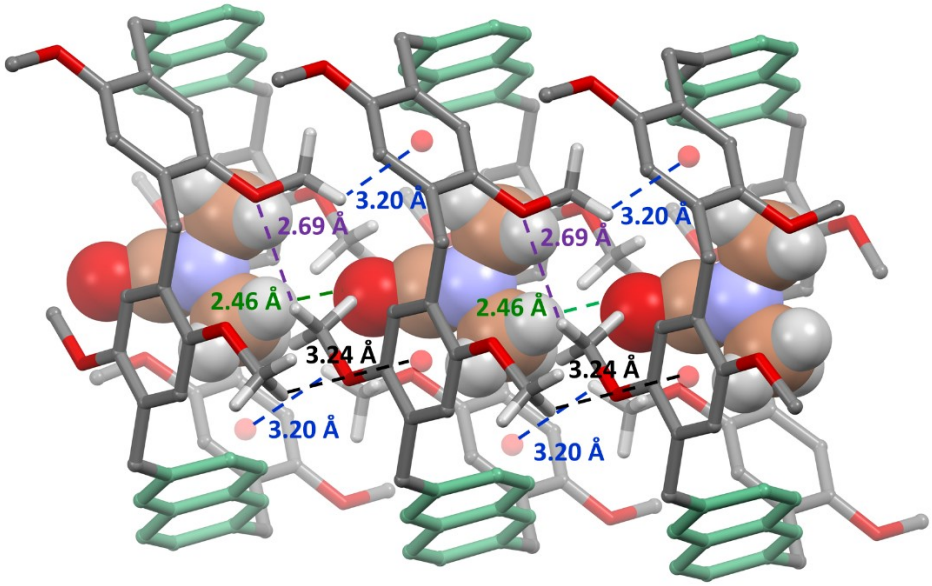

Fig. S15. The non-covalent interactions of the self-assembled supramolecular polymer based on **[2]Naph-ExP6·DMF**.

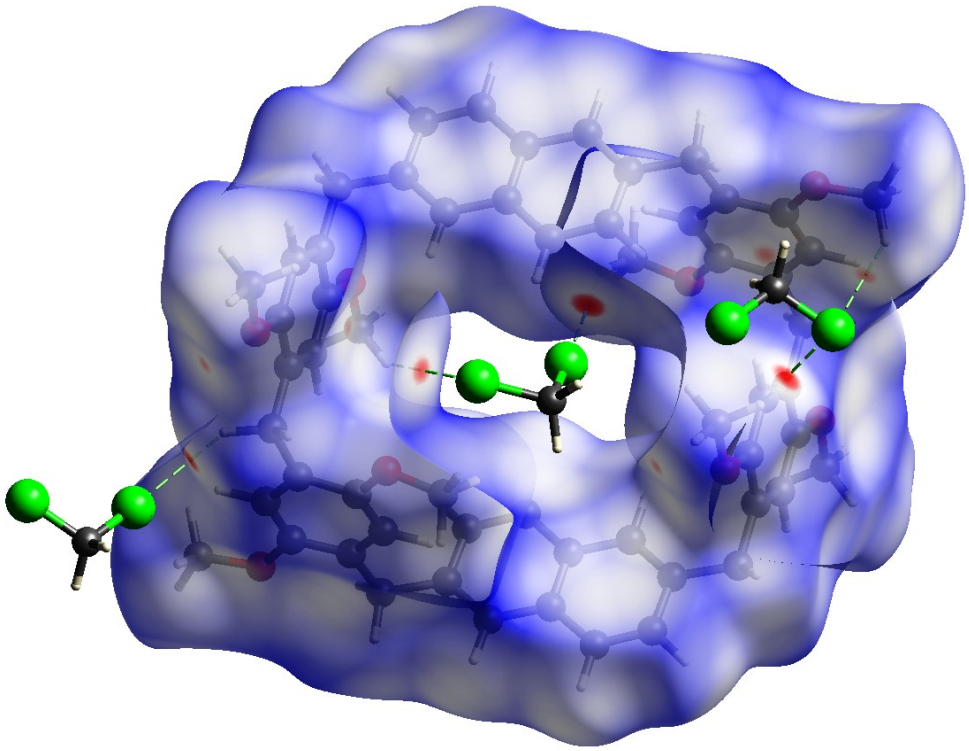

Fig. S16. Hirshfeld surfaces (dnorm) of [2]Naph-ExP6•CH_2Cl_2 showing the dichloromethane-macrocycle interactions both inside and outside the cavity

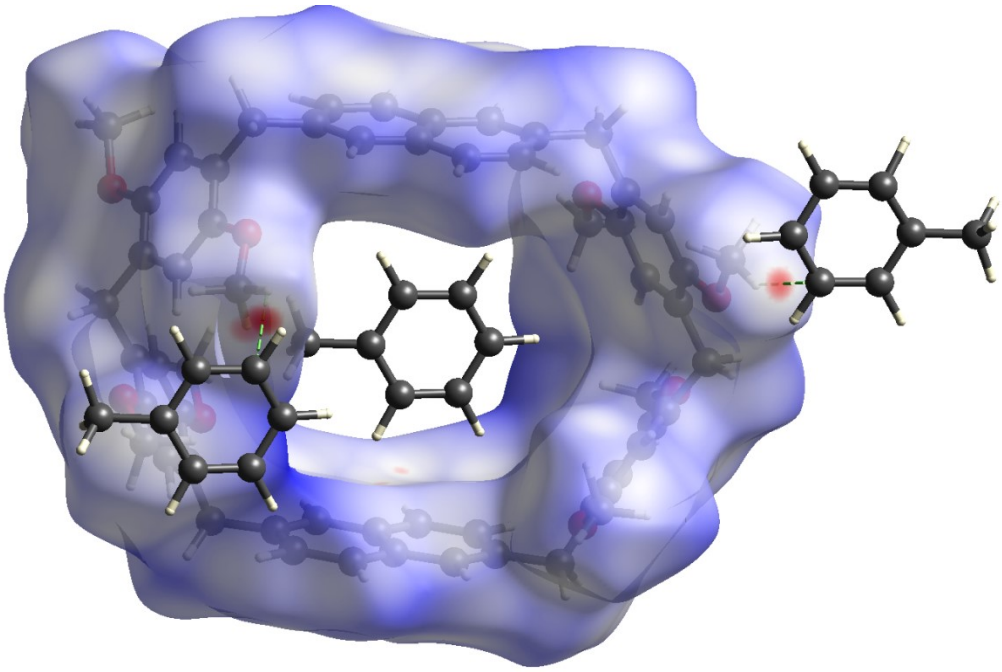

Fig. S17. Hirshfeld surfaces (dnorm) of [2]Naph-ExP6•PhMe showing the toluene-macrocycle interactions both inside and outside the cavity.

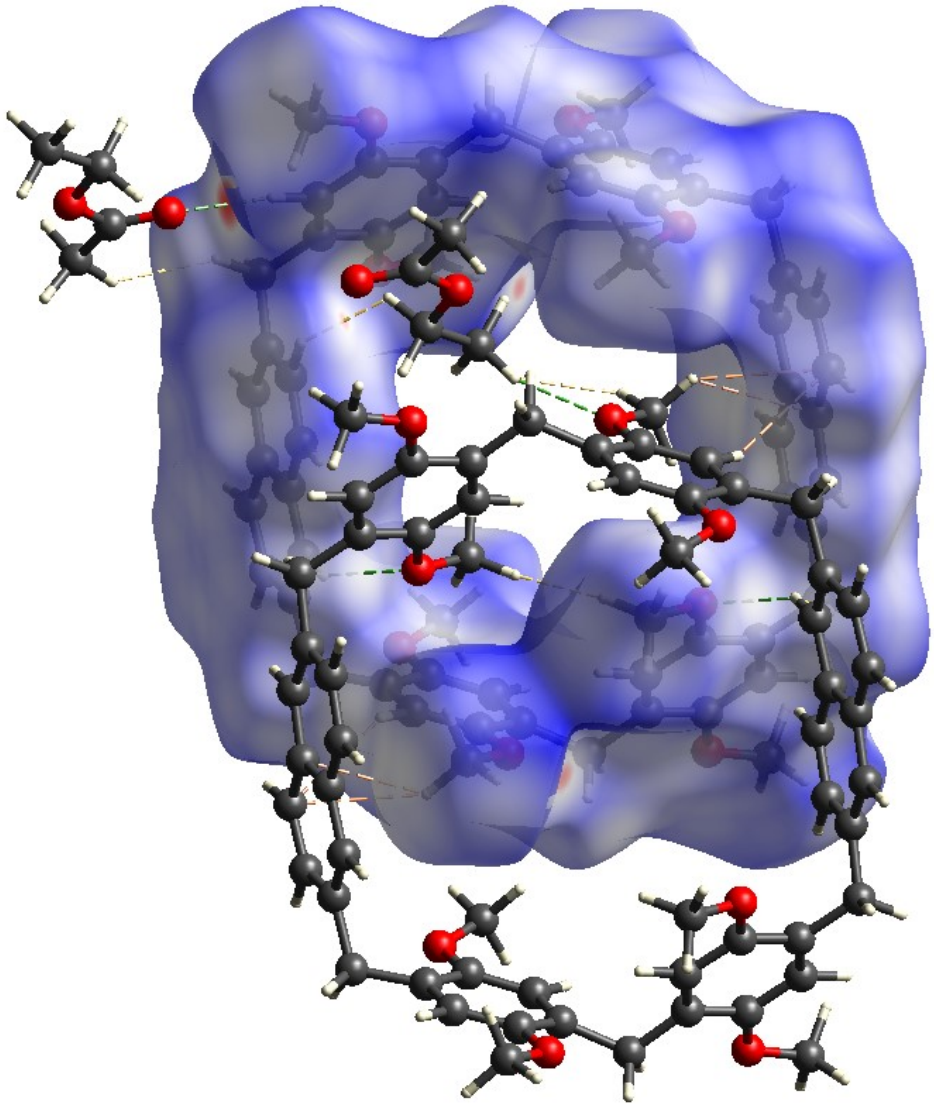

Fig. S18. Hirshfeld surfaces (dnorm) of **[2]Naph-ExP6•EtOAc** showing the ethylacetate-macrocycle interactions both inside and outside the cavity. The interpenetration of methoxy groups from an adjacent [2]Naph-ExP6 molecule into the macrocyclic cavity, accompanied by subsequent noncovalent interactions within the cavity, is also evident.

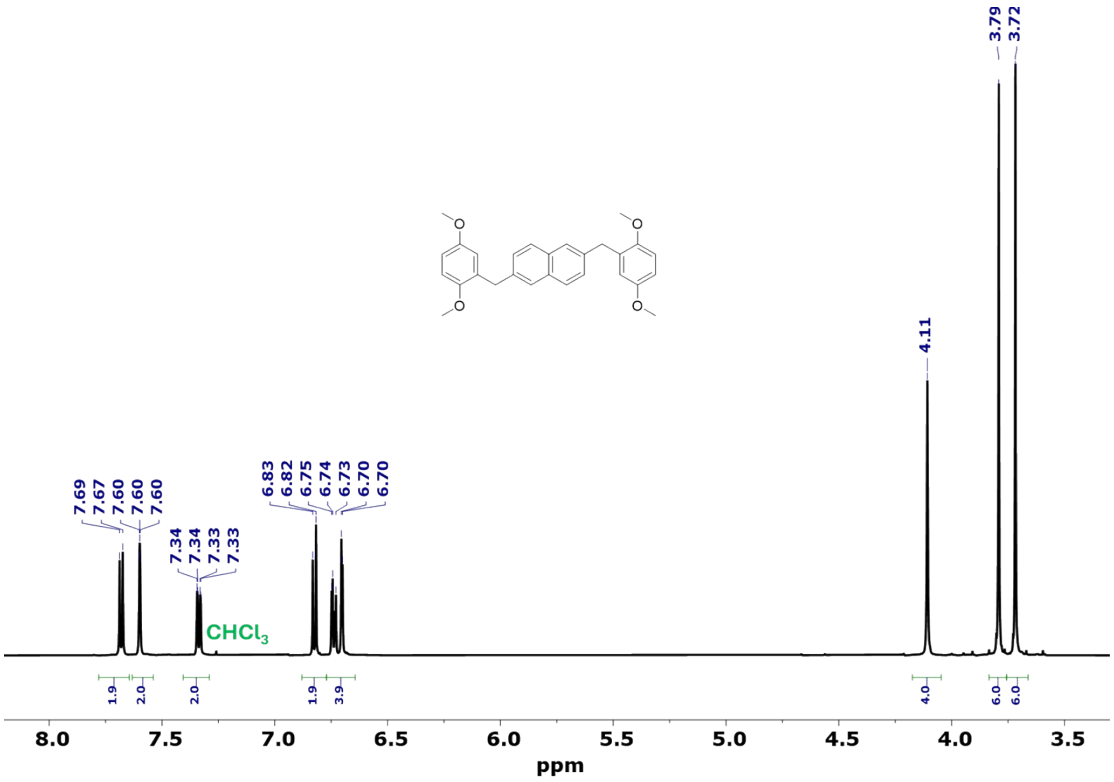

Fig. S19. ^{1}H NMR spectrum (600 MHz, $CDCl_3$) of 2,6-bis(2,5-dimethoxybenzyl)naphthalene.

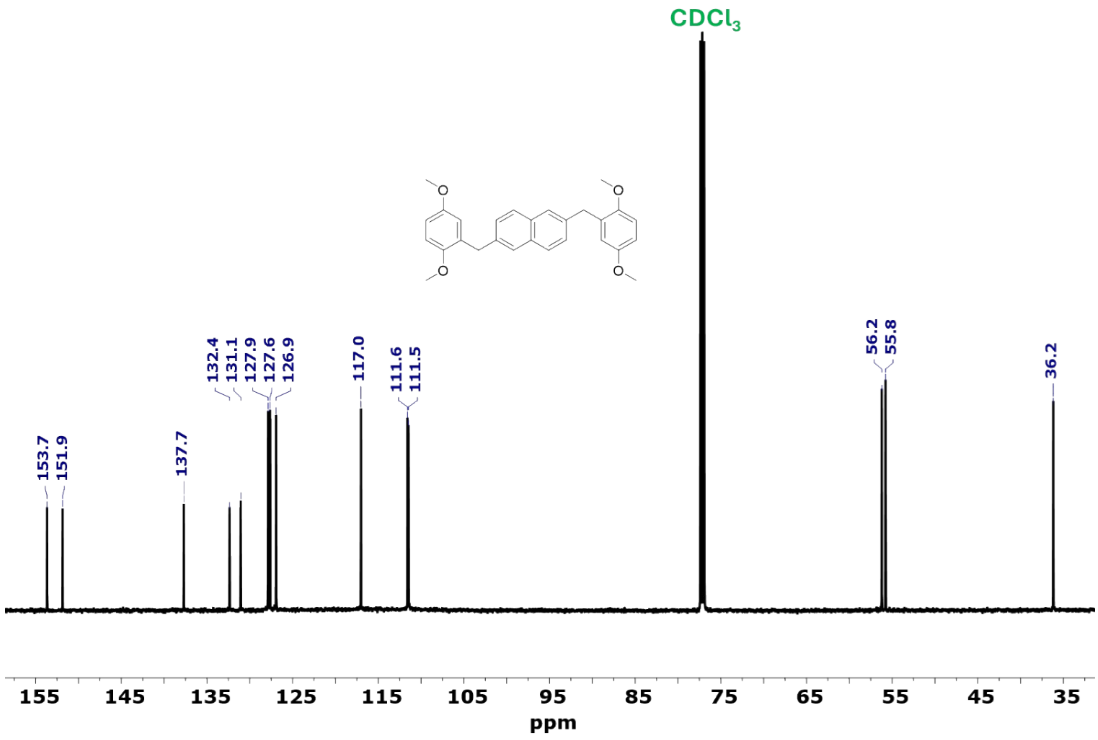

Fig. S20. ^{13}C NMR spectrum (150 MHz, $CDCl_3$) of 2,6-bis(2,5-dimethoxybenzyl)naphthalene.

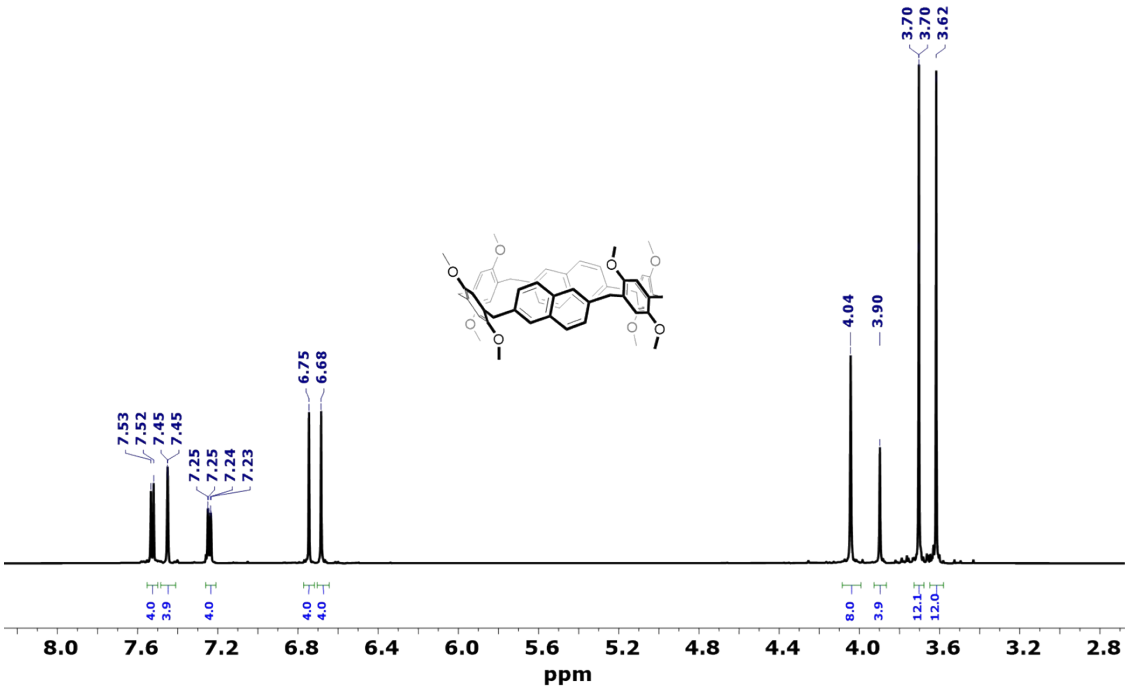

Fig. S21. ^{1}H NMR spectrum (600 MHz, $CDCl_3$) of [2]naphthyl-extended pillar[6]arene (**[2]Naph-ExP6**).

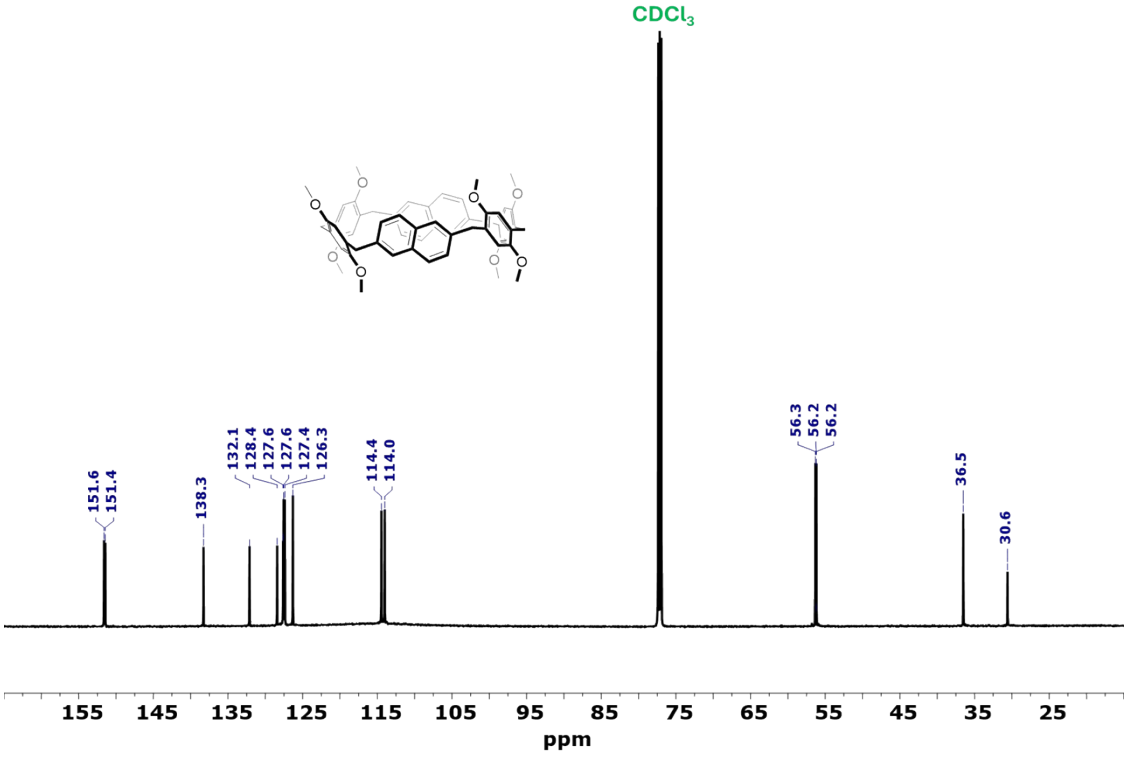

Fig. S22. ^{13}C NMR spectrum (150 MHz, $CDCl_3$) of [2]naphthyl-extended pillar[6]arene (**[2]Naph-ExP6**).

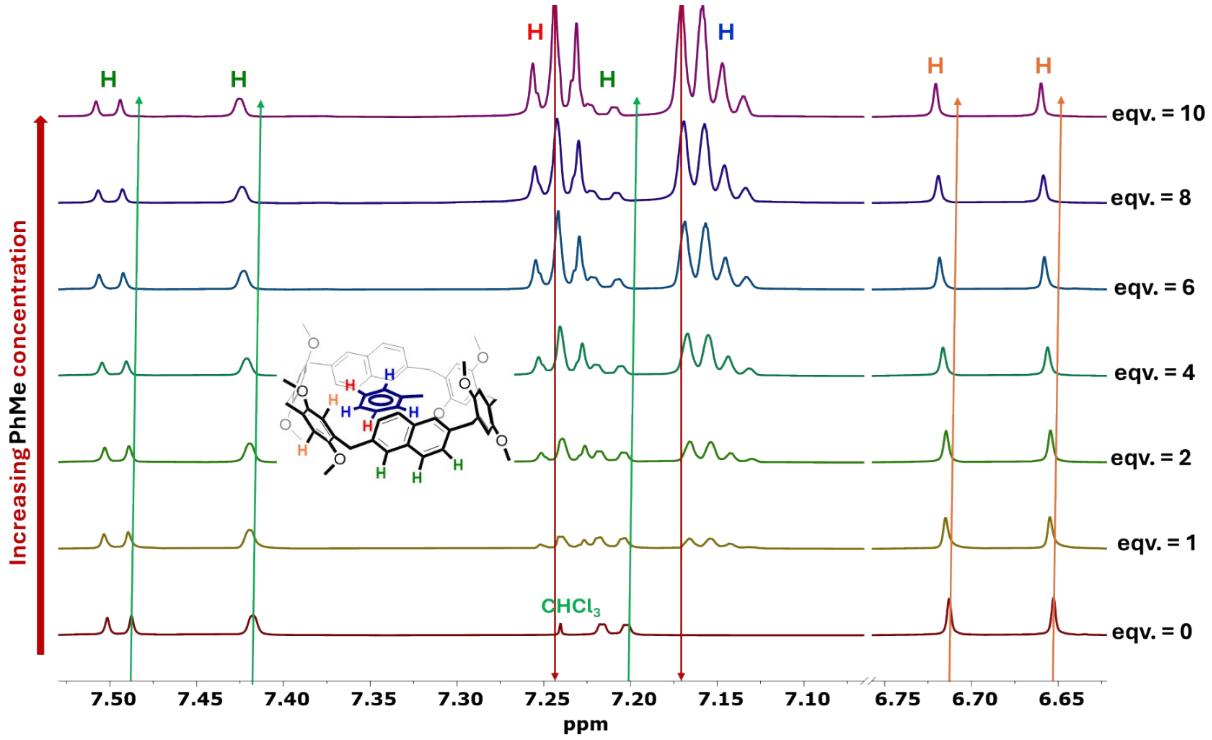

Fig. S23. Expanded aromatic region ^{1}H NMR spectra (600 MHz, $CDCl_3$) measured upon incremental addition of the guest PhMe (0 → 10 eq) to a solution of [2]naphthyl-extended pillar[6]arene (5 mM) at 298 K.

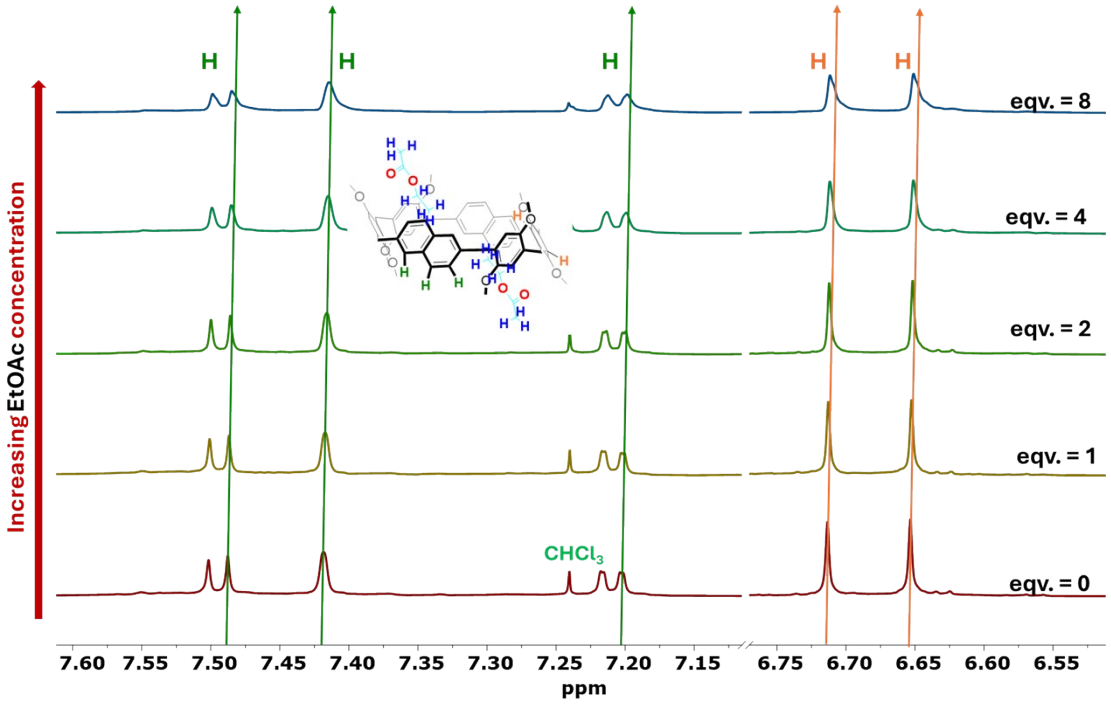

Fig. S24. Expanded aromatic region ^{1}H NMR spectra (600 MHz, $CDCl_3$) measured upon incremental addition of the guest EtOAc (0 → 8 eq) to a solution of [2]naphthyl-extended pillar[6]arene (5 mM) at 298 K.

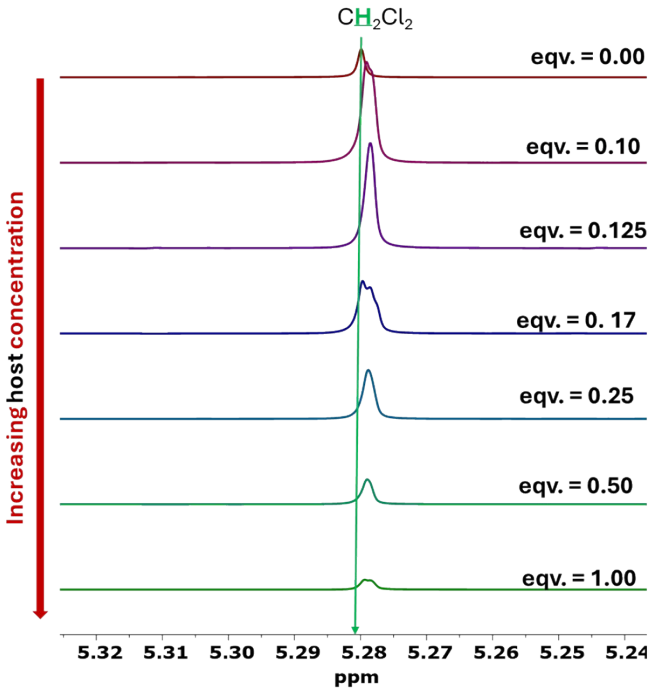

Fig. S25. ^{1}H NMR spectra (600 MHz, $CDCl_3$) of dichloromethane measured upon incremental addition of the guest DCM (0 → 10 eq) to a solution of [2]naphthyl-extended pillar[6]arene (5 mM) at 298 K.

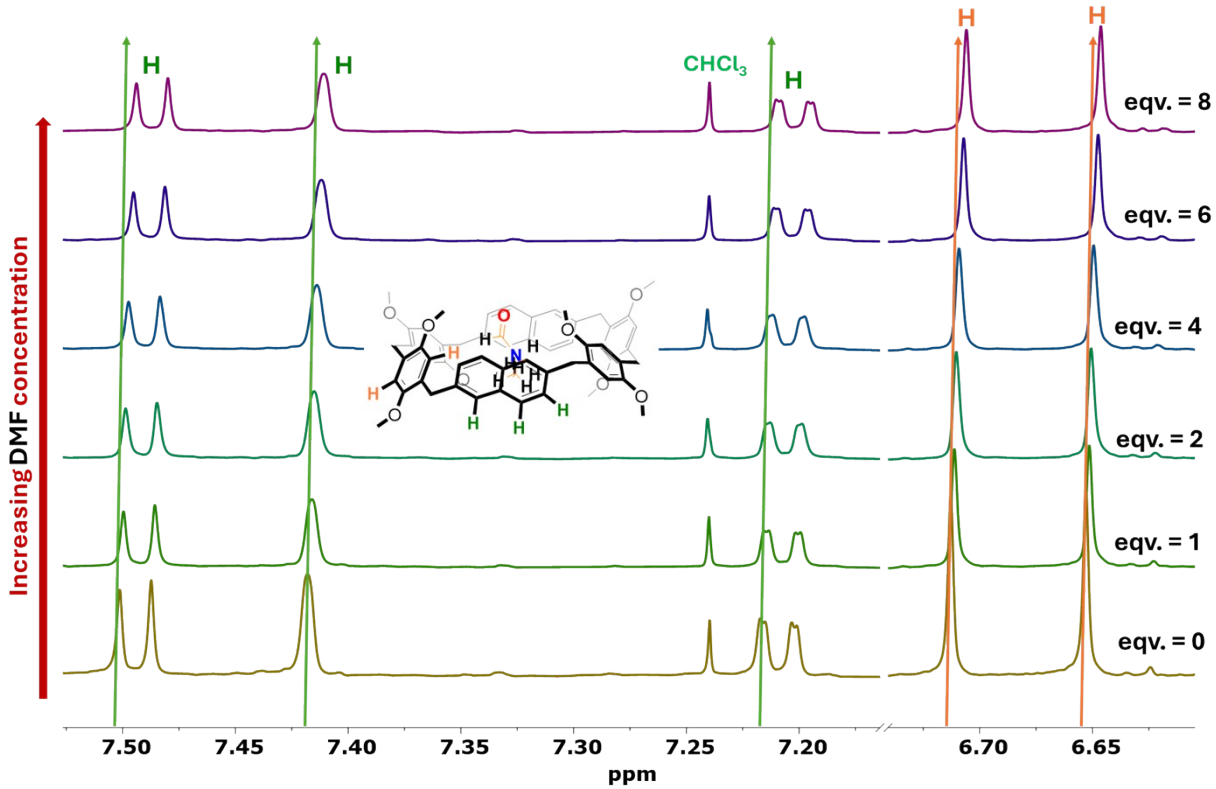

Fig. S26. Expanded aromatic region ^{1}H NMR spectra (600 MHz, $CDCl_3$) measured upon incremental addition of the guest DMF (0 → 8 eq) to a solution of [2]naphthyl-extended pillar[6]arene (5 mM) at 298 K.

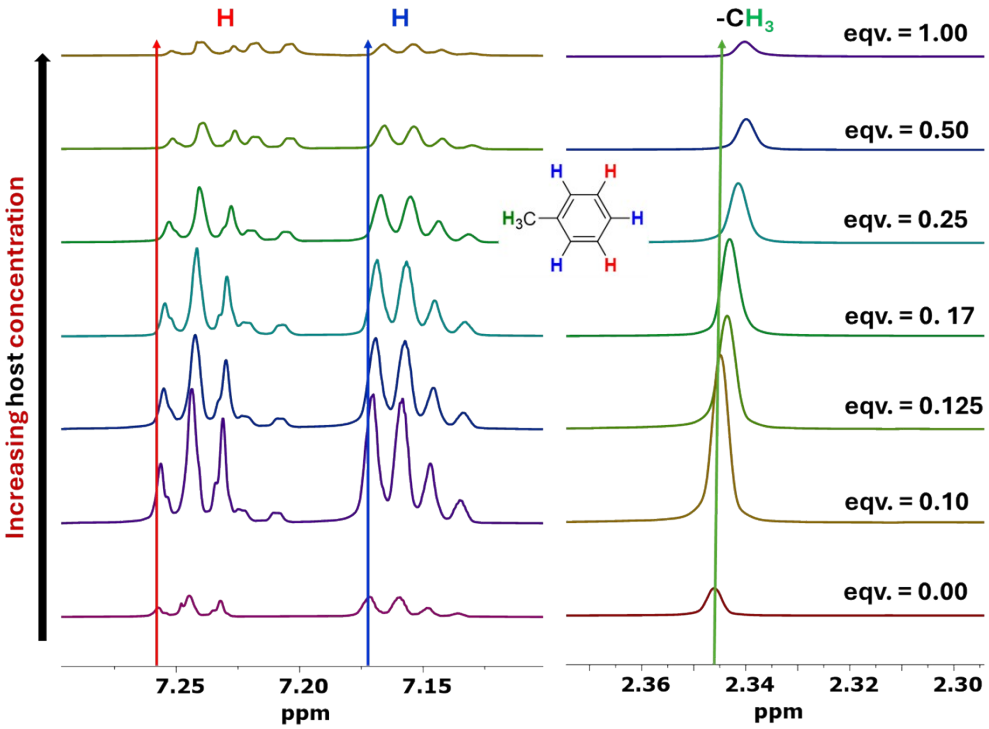

Fig. S27. Expanded ^{1}H NMR spectra (600 MHz, $CDCl_3$) of the guest (**PhMe**) measured upon incremental addition of the guest PhMe (0 → 10 eq) to a solution of [2]naphthyl-extended pillar[6]arene (5 mM) at 298 K.

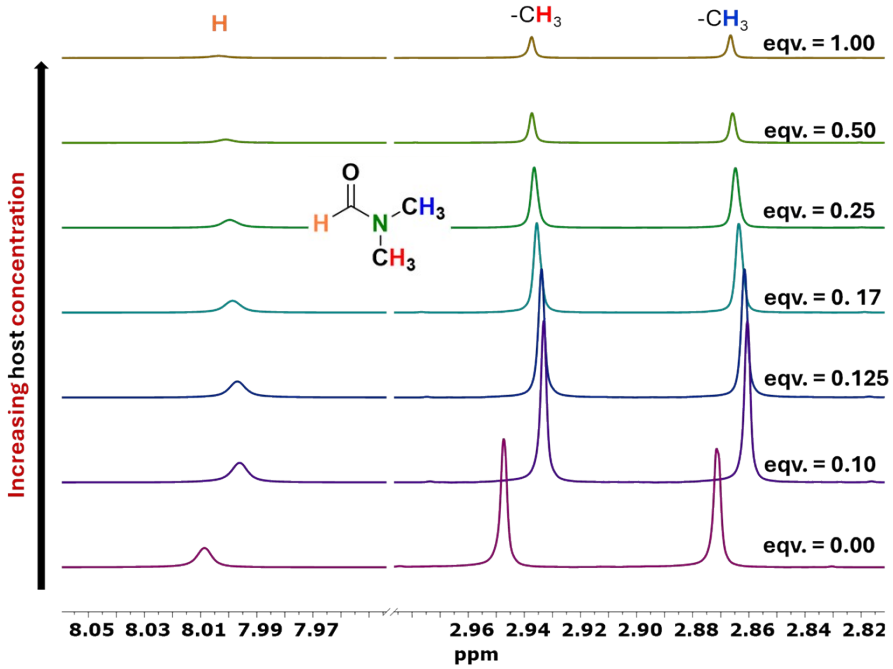

Fig. S28. Expanded ^{1}H NMR spectra (600 MHz, $CDCl_3$) of the guest (**DMF**) measured upon incremental addition of the guest DMF (0 → 10 eq) to a solution of [2]naphthyl-extended pillar[6]arene (5 mM) at 298 K.

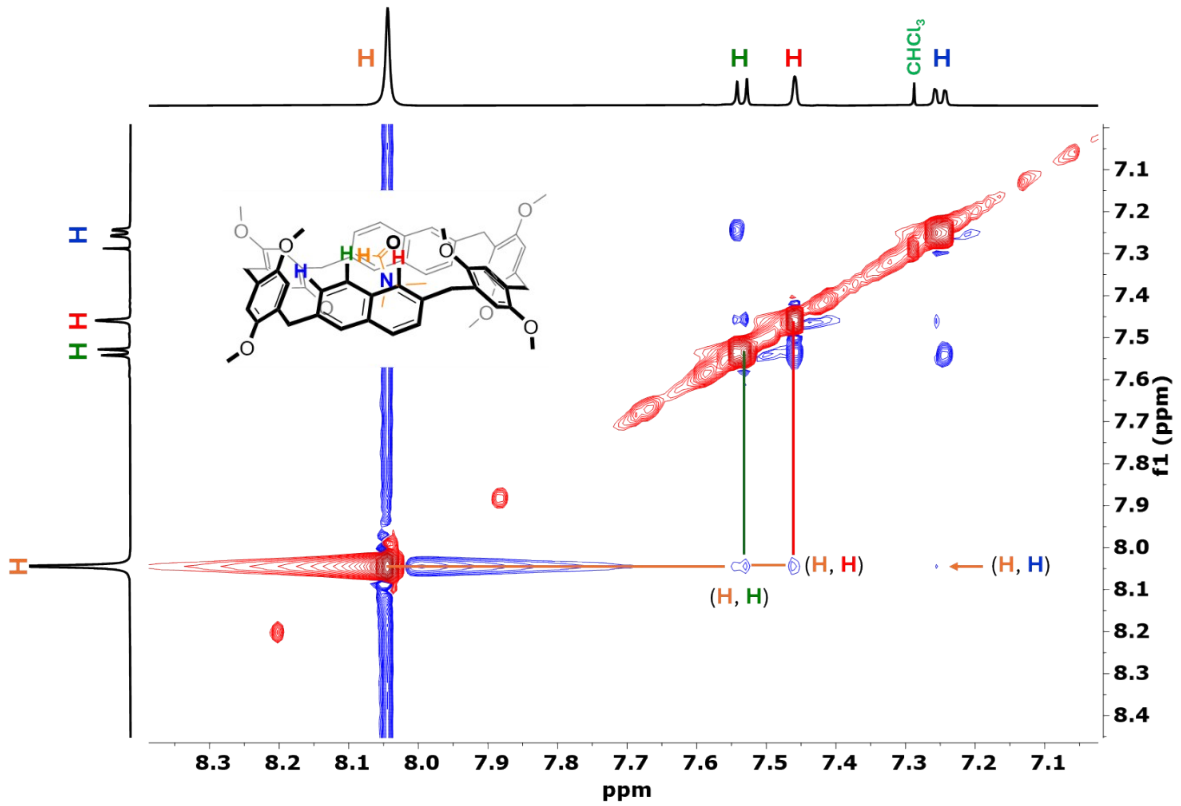

Fig. S29. Expanded ^{1}H-^{1}H ROSY NMR spectrum (600 MHz, $CDCl_3$) of inclusion complex formed between [2]naphthyl-extended pillar[6]arene and **DMF** (5 mM) recorded at 298 K.

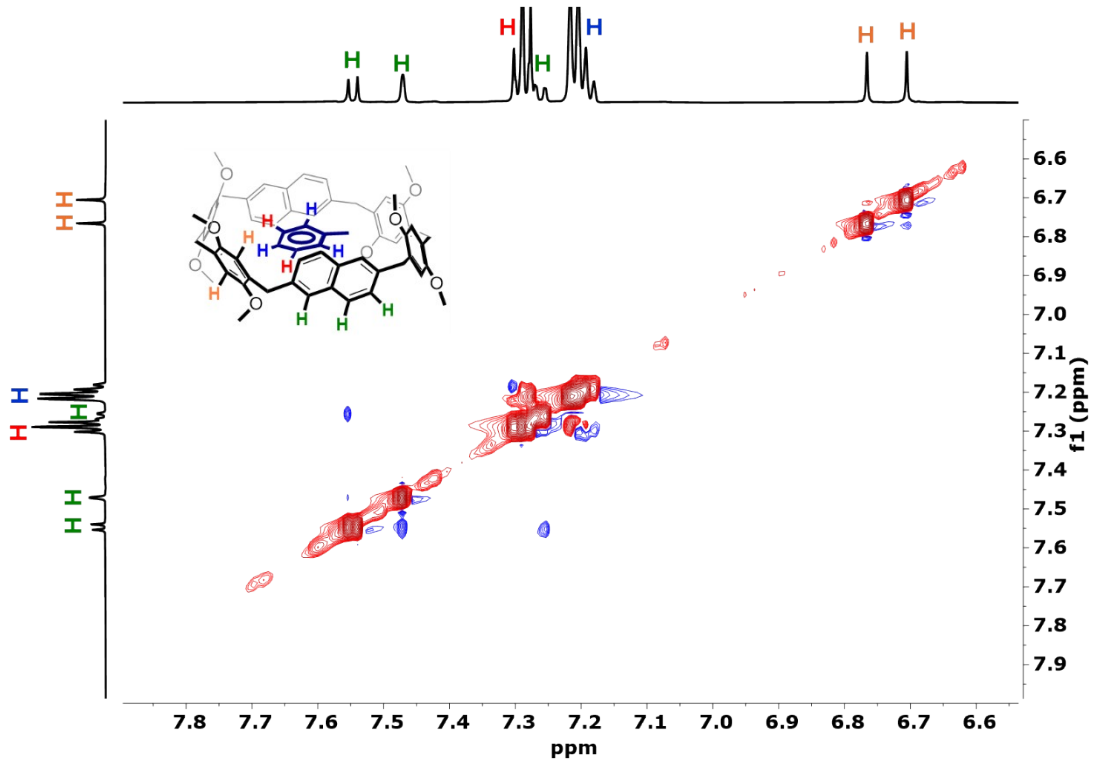

Fig. S30. Expanded ^{1}H-^{1}H ROSY NMR spectrum (600 MHz, $CDCl_3$) of inclusion complex formed between [2]naphthyl-extended pillar[6]arene and **PhMe** (5 mM) recorded at 298 K.